Chapter 104
Spin-Resolved Photoemission Electron Microscopy

Keiki Fukumoto

Keywords Magnetic domains · Imaging · Synchrotron X-ray

104.1 Principle

When the order of magnetic spins is locally different, it is the so-called magnetic domains. Domain structures can be randomly formed or it can be also formed by the competition of magnetic energies such as magnetic dipole, exchange, anisotropy, and Zeeman energies. Photoemission electron microscopy (PEEM) with polarized sources, such as spin-polarized electron beam [1], polarized UV light [2], linearly [3] or circularly [4] polarized X-rays, is one of the techniques to image magnetic domain structures (spin-resolved PEEM: SR-PEEM). In particular, a combination of PEEM with X-ray magnetic circular dichroism (XMCD-PEEM) for ferromagnetic domains is one of the most developed methods, which will be introduced in this chapter.

The details of XMCD will be described elsewhere in this book, therefore, briefly here. A micron-sized ferromagnetic material with relatively weak magnetic anisotropy and exchange energies (i.e., FeNi alloy) creates a magnetic closure domain to reduce the dipole energy, as schematically shown in Fig. 104.1a, in which the magnetization directions are indicated by black arrows. A blue thick arrow indicates the incidence of circularly polarized X-ray (CPX), and its spin direction is given by a gray arrow. Figure 104.1b shows conceptual drawing of X-ray absorption spectra (XAS) in regions A and B obtained by CPX around the Fe *2p* absorption edge. The *2p* edge splits into two ($2p_{3/2}$ and $2p_{1/2}$) by the strong spin–orbit interaction. The red curve in Fig. 104.1b is XAS in region A, where the magnetization direction is more parallel compared with other areas. On the other hand, the blue curve in Fig. 104.1b is from region B with more antiparallel configuration. The difference of photoab-

K. Fukumoto (✉)
Institute of Materials Structure Science, High Energy Accelerator Research Organization (KEK), Ibaraki, Japan
e-mail: keiki@post.kek.jp

© Springer Nature Singapore Pte Ltd. 2018

The Surface Science Society of Japan (ed.), *Compendium of Surface and Interface Analysis*, https://doi.org/10.1007/978-981-10-6156-1_104

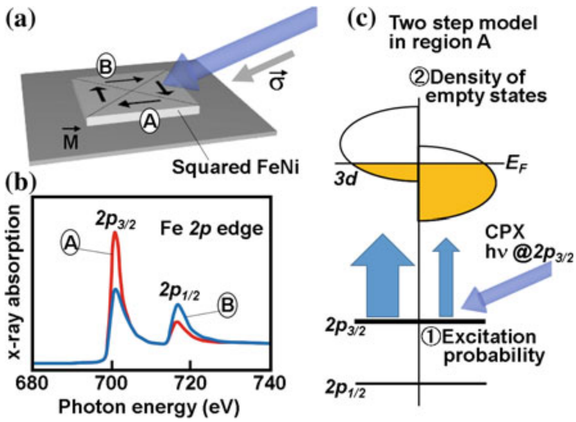

Fig. 104.1 Brief introduction of XMCD

sorption, the XMCD contrast, can be explained by two-step model using the $2p_{3/2}$ edge in Fig. 104.1c. The first step is the difference of excitation probabilities depending on the angle between spin direction of CPX and magnetization directions. The second step is the ratio of detection of the excited spin up and down electrons defined by *3d* empty states. By taking into account these two steps, the transition probabilities from $2p_{3/2}$ core level into *3d* valence level are defined. Using PEEM, locally different XMCD signal can be imaged.

104.2 Features

- Spatial resolution is a few tens of nm.
- PEEM should be equipped in a high vacuum or in an ultrahigh vacuum chamber.
- Microspectroscopic XMCD-PEEM allows to pixel by pixel analysis of spin and orbital moments using sum rule.
- By the virtue of using synchrotron X-ray, magnetic domains can be imaged with element selectively.
- Using the pulse feature of synchrotron X-ray and synchronizing it to external (magnetic) field pulses, dynamics of magnetic domain can be imaged.

104.3 Instrumentation

The contrast of PEEM images reflects locally different photoemitted electron intensities, which depend on surface morphology, workfunction, absorption coefficient, and also electron density of states. The photoemitted electrons are accelerated toward an objective lens by the potential difference to the sample. The

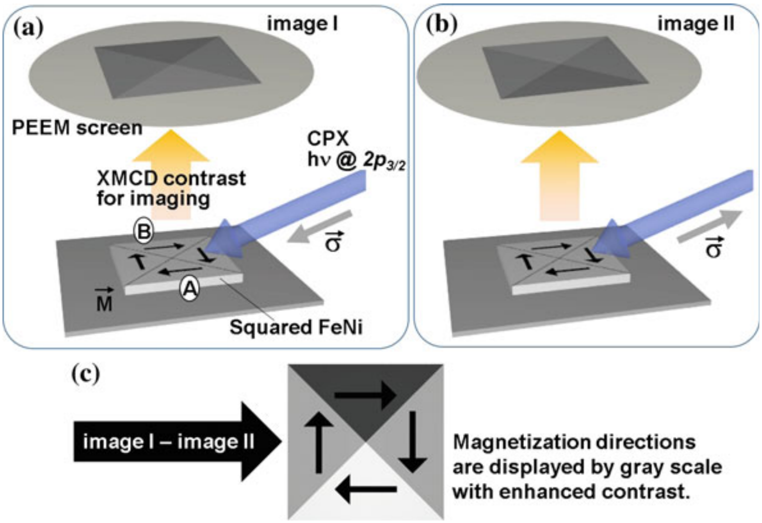

Fig. 104.2 Procedure to create a magnetic domain structure image

extracting voltage is approximately 20 kV in 2 mm for the high-resolution mode. After passing through electrostatic or magnetic lenses, the number of electrons is amplified by channel plates and converted to photons by a fluorescence screen to image by a CCD camera. The lateral resolution of PEEM is on the tens of nm defined by chromatic and spherical aberrations.

Figure 104.2 shows one procedure to create a magnetic domain image by XMCD-PEEM. Here assuming again that the sample is a square-shaped micronsize and the photon energy of CPX is tuned at the Fe $2p_{3/2}$ edge. Figure 104.2a and b illustrates the imaging of magnetic domain structures using PEEM with reversed grayscale contrasts by left and right CPXs. Taking difference of two PEEM images obtained by left and right CPX, the magnetic contrast will be enhanced (Fig. 104.2c).

104.4 Applications

104.4.1 Estimation of Spin and Orbital Moments with Spatial Resolution

One pioneer work estimating the spin and orbital moments with element selectively in sub-micron spatial resolution using XMCD-PEEM has been reported in Ref. [4], for which the sample was an epitaxially grown Co/Ni double layer on a Cu(001) surface. Co and Ni layers were prepared as a crossed wedge with slope rotated by 90° with respect to each other, as schematically drawn in Fig. 104.3a. In the region of interest in

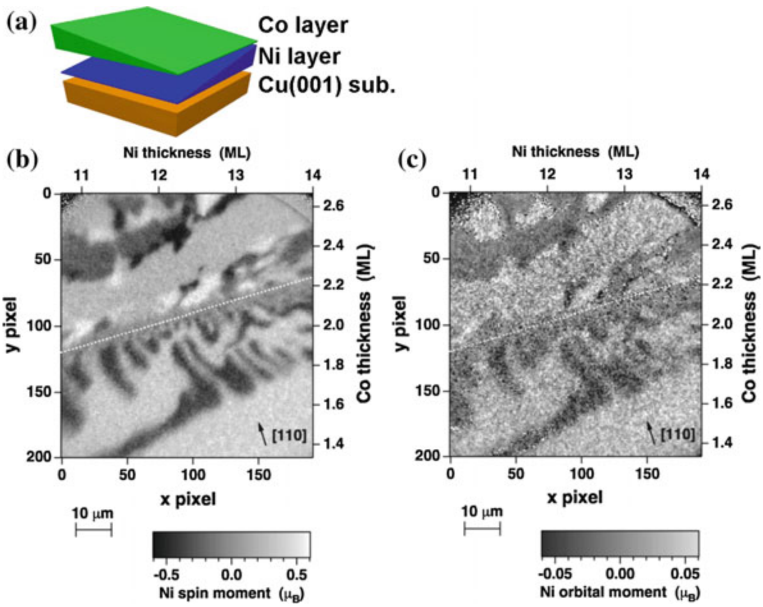

Fig. 104.3 **a** is a schematic drawing of a crossed wedge Co/Ni layer on a Cu (001) surface. **b** and **c** are maps of spin and orbital moments, respectively [4]. Figure 104.3 adapted with permission from Ref. [4] Copyrighted by the American Physical Society

this study, the thickness range for the Co and Ni layers were 1.4 to 2.6 monoatomic layer (ML) and 11 to 14 ML, respectively. The spin direction of the Co/Ni layer was determined by the competition of thickness dependent magneticrystalline anisotropy energies of these two layers. They were in-plane and out-of-plane on the upper and bottom parts of the white dotted line in the figure.

PEEM images were taken at around the Ni *2p* absorption edge with arbitrary energy steps with both left and right circularly polarized X-rays, and an XMCD spectrum (difference of the two spectra) was obtained from each pixel. By analyzing the data set using sum rule, the maps of spin and orbital moments have been successfully obtained and shown in Fig. 104.3b and c, respectively. The thicknesses of Ni and Co layers were given at the top and right axes, respectively.

Figure 104.3b gives also the magnetization directions, in which different features of magnetic domain structures were recognized in the upper and lower parts separated by the white dotted line. The bottom part of the image shows two grayscale contrasts with out-of-plane magnetizations, and the magnetizations were up or down to the paper plane. The spin direction switches from out-of-plane to in-plane direction with increasing the Co thickness and decreasing the Ni thickness. The upper part shows four contrasts with in-plane <110> easy axis. The spin moment was uniform in whole area; however, the orbital moment drastically changed when spin direction switched from in-plane to out-of-plane across the white dotted line. By pixel by pixel analysis of microspectroscopic XMCD-PEEM images on the crossed wedge sample, the spin and orbital moments relating to the magnetocrystalline anisotropy have been successfully estimated.

The measurements have been performed at the twin helical undulator beamline for BL25SU of SPring-8.

104.4.2 Dynamics of Magnetic Domain Structures

Pulsed feature of synchrotron X-ray is suitable for time-resolved experiments with a pump and probe scheme. Here, an example of imaging the dynamics of magnetic domain structures by synchronizing CPX pulses with magnetic field pulses will be introduced [5]. The experiments were performed at the soft X-ray beamline BL25SU of SPring-8. Diagram of experimental setup of Ref. [5] is shown in Fig. 104.4. One filling pattern of electron bunches of the storage ring was a combination of one train bunch and 2.92 MHz isolated single bunches. Magnetic field pulses created by shining femtosecond laser pulses to a fast photodiode were synchronized to the isolated bunches. Photoemittted electrons by the bunch train were blocked by reducing the channel plate voltage. A sample was a disk-shaped FeNi with the dimension of the diameter of 6 um and the thickness of 100 nm, which had a magnetic vortex structure and an XMCD-PEEM image of which is shown in Fig. 104.5d. The grayscale continuously changes around the center of the disk. Appling magnetic field pulse pushes the vortex core close to the edge of the disk, and subsequently, the core shows damped oscillation back to the center of the disk. Temporal motion of the core is plotted in Fig. 104.5g. XMCD-PEEM images were stored at each delay between CPX pulses and magnetic field pulses from −2 to

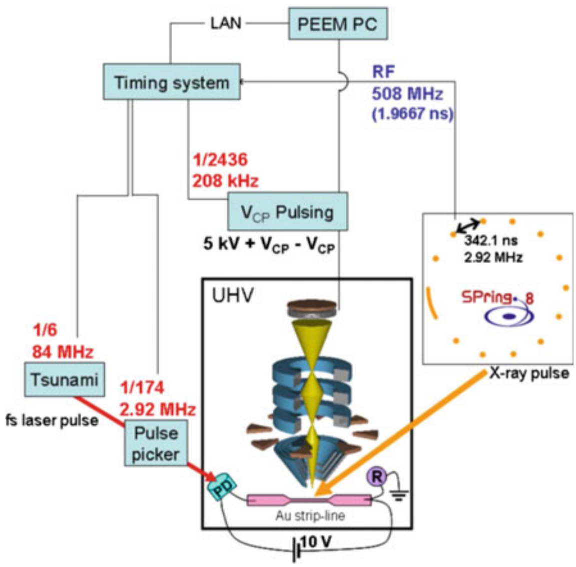

Fig. 104.4 Diagram of time-resolved XMCD-PEEM experiments [5]

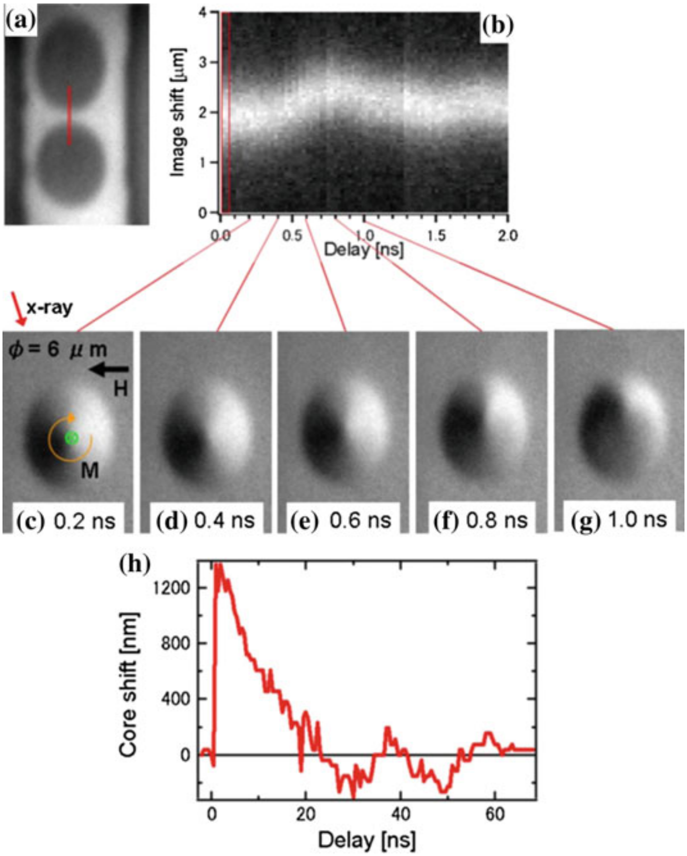

Fig. 104.5 Time evolution of magnetic domain structure in a disk-shaped FeNi [5]

78 ns with 0.5 ns step. To create one image at each delay, the photoemission signal with approximately 300,000 pulses was accumulated. Therefore, the dynamics has to be repeatable on each magnetic field pulse.

References

1. Duden, T., Bauer, E.: Magnetization wrinkle in thin ferromagnetic films. Phys. Rev. Lett. **77**, 2308–2311 (1996)
2. Marx, G.K.L., Elmers, H.J., Schonhens, G.: Magneto-optical linear dichroism in threshold photoemission electron microscopy of polycrystalline Fe films. Phys. Rev. Lett. **84**, 5888–5891 (2000)
3. Nolting, F., Scholl, A., Stohr, J., Seo, J.W., Fompeyrine, J., Seigwart, H., Locquet, J.-P., Anders, S., Luning, J., Fullerton, E.E., Toney, M.F., Scheinfein, M.R., Padmore, H.A.: Direct observation of the alignment of ferromagnetic spins by antiferromagnetic spins. Nature **405**, 767–769 (2000)

4. Kuch, W., Gilles, J., Kang, S.S., Imada, S., Suga, S., Kirschner, J.: Magnetic-circular-dichroism microspectroscopy at the spin reorientation transition in Ni (001) films. Phys. Rev. B **62**, 3824–3833 (2000)
5. Fukumoto, K., Matsushita, T., Osawa, H., Nakamura, T., Muro, T., Arai, K., Kimura, T., Otani, Y., Kinoshita, T.: Construction and development of a time-resolved x-ray magnetic circular dichroism photoelectron emission microscopy system using femtosecond laser pulses at BL25SU SPring-8. Rev. Sci. Instrum. **79**, 063903–063907 (2008)